Rotating Modons over Isolated Topographic Features

RICHARD P. MIED

Center for Advanced Space Sensing, Naval Research Laboratory, Washington, D.C.

A. D. KIRWAN, JR.

Center for Coastal Physical Oceanography, Old Dominion University, Norfolk, Virginia

G. J. LINDEMANN

Center for Advanced Space Sensing, Naval Research Laboratory, Washington, D.C.

(Manuscript received 28 October 1991, in final form 10 March 1992)

ABSTRACT

In this paper steadily rotating modons that are trapped over topographic features with finite horizontal length scales are described. The quasigeostrophic equation over topography is transformed to a frame rotating with angular frequency ω, and steady solutions are sought that decay monotonically outside of a circle of radius, $r = r_a$. These conditions are imposed upon an isolated seamount or depression of the form $\eta = h_0[1 - (r/r_b)^m]$ (and $\eta = 0$ for $r \geq r_b$) with primary focus on the $m = 2$ case. Two different scenarios result from this choice of topography and correspond to $r_a/r_b = \alpha^{1/2} \geq 1$ or $\alpha^{1/2} \leq 1$. There are three solution regions compared with the usual two for rectilinear modons. Both scenarios result in a countable infinity of both radial and azimuthal modes. In addition, it is found that an axisymmetric flow with a particular form but arbitrary amplitude can be added to the basic modon multipole solutions. The angular frequency is then found as a function of α and this axisymmetric flow amplitude. Topographically trapped rotating modons can spin clockwise or anticlockwise.

1. Introduction

Modons are exact solutions to the nonlinear quasigeostrophic potential vorticity equation. Classical solutions have two piecewise continuous regions in which the potential vorticity and the streamfunction are uniquely related. In a dissipationless ocean with a flat bottom, they translate steadily without change in shape or strength. Larichev and Reznik (1976) and Stern (1975) studied the case of barotropic beta-plane symmetric-dipole modons with the streamfunction and potential vorticity linearly related, and with a circular dividing streamline between the inner and outer regions. These studies established that modons propagate eastward at any speed, or westward at speeds greater than the long-wave speed.

The basic modon concept has been extended in a number of ways. Berestov (1978) discovered that a sort of three-dimensional modon can exist in a stratified fluid and showed that, in principle, both two- and three-dimensional modons with three distinct radial domains were possible. Flierl et al. (1980) developed a wide variety of solutions for a two-layer ocean and introduced the idea of a rider: that is, an axisymmetric (monopolar) vortex superimposed on the azimuthal part (the modon) that has a specific functional form but an arbitrary amplitude.

Although all of the works cited thus far deal with modons on a beta plane, the concept is evidently quite robust and can be readily adapted to different geometries as well. Both Tribbia (1984) and Verkley (1984) have shown that modons may exist in spherical geometry. Nof (1990) has extended the idea to produce stationary modons in a circular gamma plane (where f has a quadratic spatial dependence), which has obvious relevance to polar regions.

Because these wave forms are essentially nonlinear large-amplitude eddies that propagate steadily, the question arises as to which commensurately strong forcing mechanism(s) could be responsible for their generation. McWilliams and Flierl (1979) showed that a modon will arise quite readily from the nonlinear evolution of a pure baroclinic eddy in a two-layer ocean. In similar fashion, eastward-propagating modons have been observed to arise from a wide variety of initial conditions (Mied and Lindemann 1982) when oppositely signed vortices with separated centers are placed in each of two layers and allowed to evolve. Modons also can result from scenarios that do not start with eddies. For example, Flierl et al. (1983) have shown that in a rotating laboratory tank modon genesis

Corresponding author address: Dr. Richard P. Mied, Naval Research Laboratory, Code 4220, Washington, DC 20375-5000.

can result from the impulsive injection of fluid from the side into the body of the fluid. The modon consists of a vortex pair of unequal strength that propagates steadily along a curved trajectory. But the most intriguing example of modon formation has been demonstrated by McWilliams (1983), who showed that a southwest-propagating anticyclone and a northeast-propagating cyclone can collide, rapidly adjust their internal potential vorticity distributions, and "stick" together to form a modon that propagates steadily westward. A novel feature of the resulting modon is that the potential vorticity is a *nonlinear* function of the streamfunction, in contrast to the linear relation in analytical modon studies.

Modons are generally quite robust and can propagate for long periods of time without any substantial change. In fact, Swaters and Flierl (1989) have used the approximate invariance of form to perform analytical calculations for the decay of a propagating modon. Their analytic results are in agreement with numerical calculations that show that modons adjust their speed and size to compensate for the loss in strength. There may be cases, however, in which modon propagation does not proceed in a slowly varying (WKB) sense. For example, Hobson (1991) showed that westward-propagating modons do not necessarily propagate in straight lines. In that study the vortex pairs remained coherent but the trajectories showed large excursions from a straight-line path when the line of centers of the vortices was only slightly perturbed.

A more stringent test of a modon's longevity was made by McWilliams et al. (1981), who showed that when propagating in a field of externally imposed vorticity noise, modons do not disintegrate until the magnitude of the average vorticity inside the modon was of the order of the external vorticity. Still another example of a modon preserving its form while interacting with an external field is the violent modon–modon interactions described by Makino et al. (1981), McWilliams and Zabusky (1982), and Larichev and Reznik (1982, 1983). Both overtaking interactions and frontal collisions were considered. Several types of behavior were observed; however, in many experiments modons emerged from these strong interactions but with altered potential vorticity–streamfunction relations (McWilliams and Zabusky 1982; McWilliams 1983). The robustness and general resistance to disruption has also made modons attractive candidates for models of atmospheric blocks (McWilliams 1980; Verkley 1987; Haines 1989).

Of interest in the present context are the ways that barotropic modons can interact with bottom topography. Carnevale et al. (1986) examined numerically the interaction of modons with topography having a wide range of scales. They found that large-scale topography with large amplitude could cause the modon to fission but that smaller topographic amplitudes resulted in topographic steering. A similar result was obtained by Swaters (1986) who used WKB arguments to calculate analytically the path of the modon over a bottom ridge. His suggestion of the possibility of "capture" of the modon by certain topographic features is particularly relevant here.

In this work, we investigate properties of topographically trapped modons. The form of trapping we consider here does not result in a closed trajectory around the seamount, as discovered by Reznik (1985), but rather in a steady rotation of the modon over the center of the seamount. The solution for the streamfunction–potential vorticity relation will be shown to be piecewise continuous, and the resultant topographically captured modons generally require three-region solutions. Apart from these two differences, the topographically trapped modons have much in common with the more familiar rectilinear forms.

2. Formulation

The problem studied here is that of inviscid barotropic flow over an isolated submarine feature on an f plane. As the emphasis is on local topographic effects, the f-plane restriction seems reasonable. For these conditions, the potential vorticity equation for a fluid with a rigid lid is written as

$$\frac{\partial}{\partial t'} \nabla^2\Psi + J(\Psi, \nabla^2\Psi + fh/H) = 0. \qquad (1)$$

Here Ψ is the barotropic streamfunction, f is the Coriolis parameter, h describes the seamount topography above a flat bottom, H is the undisturbed ocean depth, and ∇^2 and J are the Laplacian and Jacobian operators.

In order to illustrate the essential physics with the minimum of mathematical complexity, we assume the topography radially symmetric with compact support. Thus,

$$h = F(r'), \quad r' \leq r'_b$$
$$h = 0, \qquad r' \geq r'_b. \qquad (2)$$

Here F is a smooth, monotonic function of the radius r' emanating from the center of the topographic feature and r'_b is the radial distance to its edge.

Solutions to (1) are sought of the form

$$\Psi = \Psi(r, \theta, t),$$

where $r = r'$, $\theta = \theta' - \hat{\omega}t'$, and $t = t'$. Here r' and θ' refer to a fixed circular system originating at the center of the topographic feature, while the unprimed system (r, θ) is rotating at a steady rate, $\hat{\omega}$ with respect to the fixed system. Transforming (1) into this rotating system and considering only steady solutions ($\partial/\partial t = 0$), we see that

$$J(\Psi - \hat{\omega}r^2/2, \nabla^2\Psi + fh(r)/H) = 0, \qquad (3)$$

where the Jacobian is now expressed in polar coordinates.

Equation (3) can be solved by any functional relation between the two arguments of J. In the spirit of most modon work we divide the plane into two regions, $r \leqslant r_a$ and $r \geqslant r_a$, in which the arguments in (3) are linearly related. Thus,

$$\nabla^2\Psi + fh(r)/H = -\kappa^2(\Psi - \hat{\omega}r^2/2 + \hat{Q})S(r_a - r), \tag{4}$$

where κ^2 is a separation parameter, r_a is the radius of the modon region, $\hat{Q}$ is a constant, and $S(a - x)$ is the Heaviside function such that $S = 1$ for $x < a$ and $S = 0$ for $x > a$. Butchart et al. (1989) have noted the importance of the value of the separation parameter for atmospheric blocks in zonal flow. The implication of their results for the rotary modons considered here is not addressed. This issue may be relevant to the stability of our solutions.

Boundary conditions appropriate for (4) are

$$\lim\Psi = 0, \quad r \to \infty$$
$$\lim|\Psi(r)| < \infty, \quad r \to 0. \tag{5}$$

In addition to (5), "patches" are required at $r = r_a$, r_b. Appropriate patch conditions are

$$\lim_{r \to y-}(\Psi, \partial\Psi/\partial r, \partial\Psi/\partial\theta) = \lim_{r \to y+}(\Psi, \partial\Psi/\partial r, \partial\Psi/\partial\theta), \tag{6}$$

where $y = r_a, r_b$. The first condition ensures continuity of the pressure, while the second and third imply continuity of the tangential and radial velocities.

In addition to (5) and (6) prior modon solutions of which we are aware have also assumed that the circle $r = r_a$ is a dividing streamline with a specified value. This specification ensures continuity of the riderless modon vorticity across the streamline. Of course, radially symmetric rider solutions are compatible with the basic modon solutions, and the rider vorticity need not be continuous across the dividing streamline.

Here a different approach is taken. The a priori specification is the amplitude of the axisymmetric modon rider instead of the value of a bounding streamline. This has the appealing property that the azimuthal mode is arbitrary, but the price for this flexibility is that the vorticity is not continuous across the modon boundary $r = r_a$. However, as the modon paradigm is inviscid, there is no physical or mathematical reason of which we are aware that requires continuity of the vorticity everywhere.

Convenient nondimensional scalings for r and Ψ are r_b and fr_b^2, respectively. We also introduce the following nondimensional parameters:

$$\omega = \hat{\omega}/f, \quad \beta^{-1/2} = \kappa r_b, \quad \alpha = (r_a/r_b)^2,$$
$$\gamma \equiv F(0)/H, \quad Q = \hat{Q}/fr_b^2.$$

It should be noted that the sign of γ distinguishes between mountains ($\gamma > 0$) and depressions ($\gamma < 0$). As will be seen, the solution forms are independent of the sign of γ. The analysis and example below are phrased for $\gamma > 0$, both for convenience of the reader and because this case has more potential for application.

With the above nondimensionalization, two possible scenarios emerge: $\alpha^{1/2} \leqslant 1$ and $\alpha^{1/2} \geqslant 1$. The physical significance of $\alpha^{1/2} \leqslant 1$ is that the modon region is situated entirely within the domain of the mountain (see Fig. 1). For $\alpha^{1/2} > 1$, the modon domain extends beyond the mountain region. Each scenario requires a separate analysis; however, the solutions are shown to reduce to the same form when $\alpha^{1/2} = 1$.

In either scenario there are three different flow regimes. When $\alpha^{1/2} < 1$, regime I designates the modon region centered over the mountain, while regime II refers to the annulus between the modon region and the edge of the mountain. Regime III is then the region outside the mountain. When $\alpha^{1/2} > 1$, the regime I refers to the position of the modon region centered over the mountain, while regime II comprises the annulus between the edge of the mountain and the boundary of the modon region. Regime III is then exterior to the modon region.

3. Solution

Solutions to (4) for arbitrary $F(r)$ are developed in the following. It is found that when $F(r)$ is of the form

$$F(r) = (1 - r^m)S(1 - r) \tag{7}$$

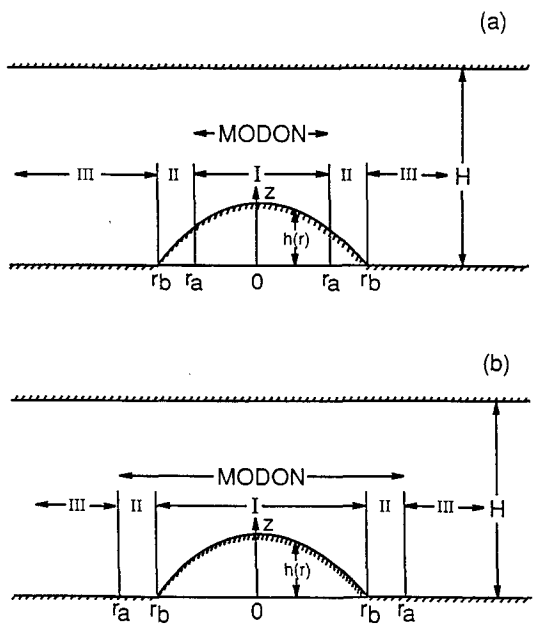

FIG. 1. A vertical slice through the dimensional topography $h = h(r)$, $r < r_a$ and $h = 0$, $r \geqslant r_b$ showing its finite lateral extent. (a) The small modon case ($r_a/r_b = \alpha^{1/2} < 1$) in which the modon radius is less than the mountain length scale. (b) The large modon case ($r_a/r_b = \alpha^{1/2} > 1$) in which the modon extends beyond the edge of the mountain.

and m is a positive, even integer, closed-form solutions are obtainable. For reasons of mathematical simplicity, the $m = 2$ case is treated in detail for both the small ($\alpha^{1/2} < 1$) and large ($\alpha^{1/2} \geq 1$) modon cases.

a. Small modon case ($\alpha^{1/2} < 1$)

The nondimensional version of (4) becomes

$$\nabla^2\Psi^I + \Psi^I/\beta + \gamma F(r) = [(\omega r^2/2 + Q)/\beta], \quad r \leq \alpha^{1/2}$$
$$\nabla^2\Psi^{II} + \gamma F(r) = 0, \quad \alpha^{1/2} \leq r \leq 1$$
$$\nabla^2\Psi^{III} = 0, \quad r \geq 1. \tag{8}$$

For each of the equations (8), we may write the solutions as a sum of particular solutions and homogeneous solutions obtained by standard separation of variables. Thus,

$$\Psi^I = G(r) + AJ_0(\beta^{-1/2}r) + \sum_{n=1} b_n^I J_n(\beta^{-1/2}r)\sin n\theta, \quad r \leq \alpha^{1/2}$$
$$\Psi^{II} = \mathrm{I}(r) + \sum_{n=1} [b_n^{II}r^{-n} + c_n^{II}r^n]\sin n\theta, \quad \alpha^{1/2} \leq r \leq 1$$
$$\Psi^{III} = \sum_{n=1} b_n^{III}r^{-n}\sin n\theta, \quad 1 \leq r, \tag{9}$$

where J_n is the Bessel function of the first kind of order n, $G(r)$ is the particular solution governed by

$$\frac{d^2G}{dr^2} + \frac{1}{r}\frac{dG}{dr} + G/\beta = \omega r^2/2\beta + Q/\beta - \gamma F(r) = \mathcal{F}(r), \tag{10}$$

and $I(r)$ is the particular solution governed by

$$\frac{d^2I}{dr^2} + \frac{1}{r}\frac{dI}{dr} + \gamma F(r) = 0. \tag{11}$$

In obtaining (9) the Y_n solutions were discarded because of (5), and as will emerge in the following, no loss of generality results from the neglect of the $\cos n\theta$ terms.

The particular solution to (10) is readily obtained by variation of parameters on the Y_0 and J_0 solutions to the homogeneous problem

$$G = (\pi/2)\left\{-J_0(\beta^{-1/2}r)\int^r x\mathcal{F}(x)Y_0(\beta^{-1/2}x)dx + Y_0(\beta^{-1/2}r)\int^r x\mathcal{F}(x)J_0(\beta^{-1/2}x)dx\right\}. \tag{12}$$

Here Y_0 is the Bessel function of the second kind and the symbol $\int^r$ denotes an indefinite integration followed by replacement of the dummy parameter x by r (Bender and Orzag 1978).

It is convenient to divide G into two parts: a dispersive component G_D that depends only upon ω and Q and a topographic part G_T that depends only on $F(r)$. Thus,

$$G = G_T + G_D.$$

After integration of (12) it is found that

$$G_D(r) = Q + \omega(r^2/2 - 2\beta) \tag{13}$$

$$G_T(r) = (\pi\gamma/2)\int^r xF(x)[J_0(\beta^{-1/2}r)Y_0(\beta^{-1/2}x) - J_0(\beta^{-1/2}x)Y_0(\beta^{-1/2}r)]dx. \tag{14}$$

The integration of (14) for functions of the form given by (7) is facilitated by a useful Bessel integral recursion formula,

$$\int^r x^{\mu+1}Z_\nu(cx)dx = \Big\{r^{\mu+1}Z_{\nu+1}(cr) + [(\mu - \nu)/c][r^\mu Z_\nu(cr)] - [(\mu^2 - \nu^2)/c] \times \int^r x^{\mu-1}Z_\nu(cx)dx\Big\}\Big/c, \tag{15}$$

where Z_ν is a Bessel function of either the first or second kind of order ν. In the present case, $\nu = 0$, and for $\mu = 0, 2, \cdots$, (15) may be written in the closed form:

$$\int^r x^{\mu+1}Z_0(cx)dx = \{(\sum_{p=0}^{\mu/2} A_p r^{2p})rZ_1(cr) + (\sum_{p=0}^{\mu/2} B_p r^{2p})Z_0(cr)\}/c, \tag{16}$$

where the A_p and B_p are readily determined recursively from (15).

Using (7) in (16) gives

$$G_T = -\beta\gamma\left\{1 + \frac{\pi}{2}\int^r x^{m+1}[J_0(\beta^{-1/2}r)Y_0(\beta^{-1/2}x) - J_0(\beta^{-1/2}x)Y_0(\beta^{-1/2}r)]dx\right\} \tag{17}$$

so that the complete particular solution $G(r)$ in region I is given by the sum of (13) and (17).

The solution for $I(r)$ in (11) is obtained by direct integration:

$$I = \Gamma_1 - \gamma\left\{\int^r \frac{dx}{x}\int^x yF(y)dy - \Gamma_2 \ln r\right\}. \tag{18}$$

The complete solution to the small modon problem is now given in principle by (9) with G_D, G_T, and I given by (13), (14) or (17), and (18). The arbitrary constants in this solution are determined by applying the boundary conditions (5) and the patching conditions (6) at the I/II and II/III boundaries. Note also that these solutions are valid for both $\gamma \gtrless 0$.

Consider first the patch of the azimuthally dependent solutions. The six patch conditions, (6), yield four linear homogeneous equations for b_n^I, b_n^{II}, c_n^{II}, and b_n^{III}:

$$b_n^I J_n(a) - b_n^{II}\alpha^{-n/2} - c_n^{II}\alpha^{n/2} = 0$$
$$b_n^I[-n\alpha^{-1/2}J_n(a) + \beta^{-1/2}J_{n-1}(a)] + n\alpha^{(-n+1)/2}b_n^{II} - n\alpha^{(n-1)/2}c_n^{II} = 0$$
$$b_n^{II} + c_n^{II} - b_n^{III} = 0$$
$$-nb_n^{II} + nc_n^{II} + nb_n^{III} = 0, \qquad (19)$$

where $a = (\alpha/\beta)^{1/2}$.

The consistency requirement that the homogeneous linear system (19) possesses a nontrivial solution is that the determinant of this system vanish. This yields

$$J_{n-1}(a) = 0. \qquad (20)$$

Thus, $a = (\alpha/\beta)^{1/2}$ is the pth root of J_{n-1}. It is then found that

$$b_n^{II} = \alpha^{n/2}J_n(a)b_n^I$$
$$c_n^{II} = 0$$
$$b_n^{III} = \alpha^{n/2}J_n(a)b_n^I. \qquad (21)$$

It is seen that (20) can only be imposed upon a single mode. Thus, (20) specifies a, so that for a given α, β is known. An attempt to enforce (20) on each $\sin n\theta$ mode in (9) results in an overspecification of a, so (20) limits the available azimuthal modes in (9) to only one. This is the reason that the $\cos n\theta$ terms were neglected earlier.

It has become commonplace in the modon literature to focus almost exclusively on dipolar solutions. Here, however, we include the higher-mode solutions because they are superficially similar to the tripoles and quad-

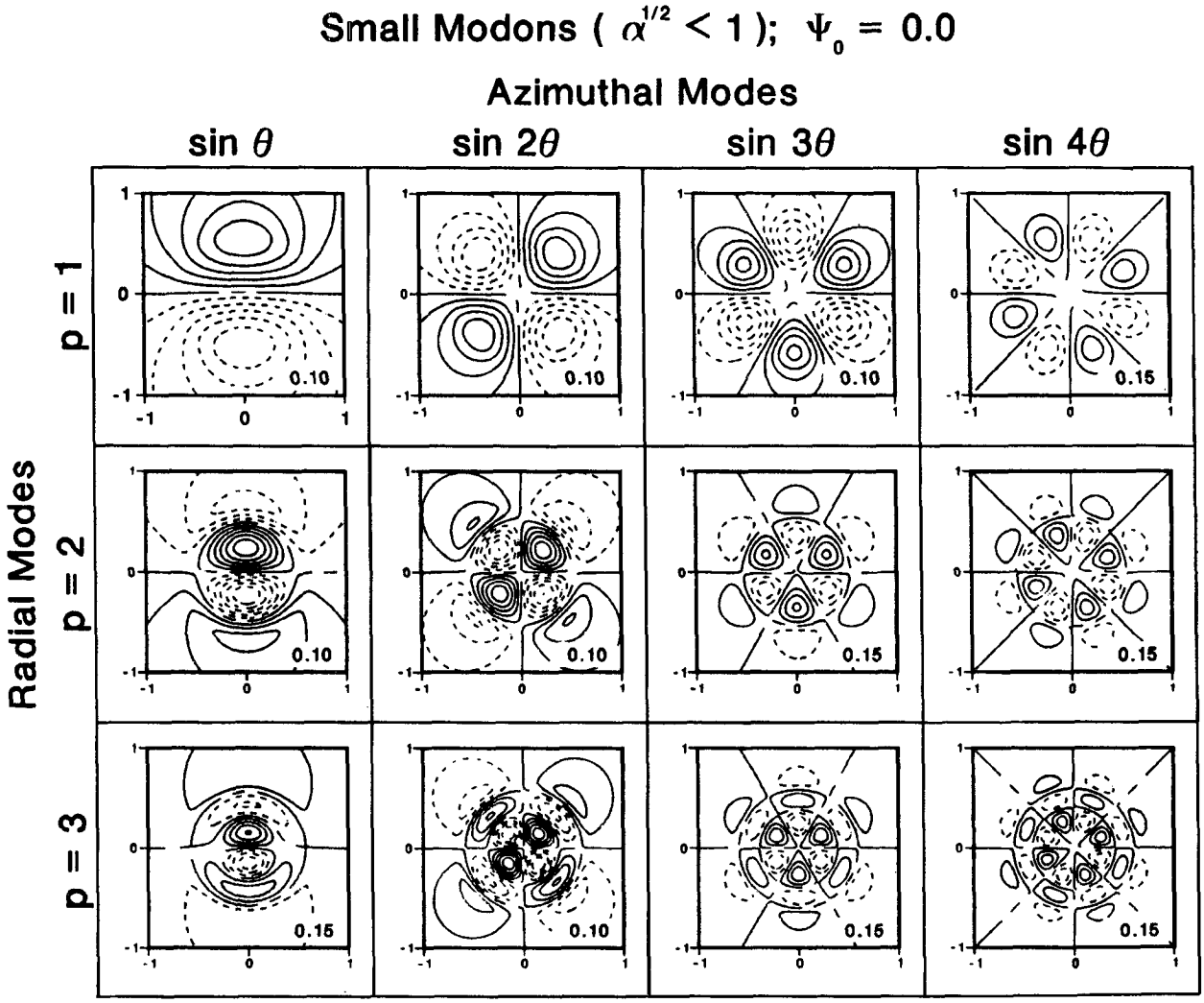

FIG. 2. Streamfunction (Ψ) contours for the small modon case ($\alpha = 0.5$) with $b_n^I = 1.0$ and $\gamma = 0.25$ and no axisymmetric part ($\Psi_0 = 0$). The first four azimuthal modes ($\sin n\theta$, $n = 1, \cdots, 4$) and the three lowest-order radial modes ($p = 1, 2, 3$) are shown. Solid lines are positive contours, dashed are negative, and solid/dashed are zero. The contour interval is given in the lower right of each panel.

rapoles observed by Kloosterzeil and van Heijst (1991) in their rotating tank experiments dealing with the stability of elongated cyclones and anticyclones.

Consider now the axisymmetric parts of the solution (9). The patch conditions (6) at $r = 1$ give [from (18)]

$$\Gamma_1 = \gamma\left[\int^1 \frac{dx}{x}\int^x yF(y)dy\right]$$
$$\Gamma_2 = \int^1 yF(y)dy \tag{22}$$

so that I may be compactly written as

$$I = \gamma\left[\int_r^1 \frac{dx}{x}\int^x yF(y)dy + \ln r\int^1 yF(y)dy\right]. \tag{23}$$

There are three conditions on $G(r)$: the two patch conditions (6) at $r = \alpha^{1/2}$ and the specification for the nontopographic part that satisfies (5) at $r = 0$:

$$G_D(0) + A \equiv \Psi_0.$$

These three conditions are used to determine Q, ω, and A. Applying these conditions to (13) and (14) yields the system:

$$Q - 2\beta\omega + A = \Psi^I(0) - G_T(0) = \Psi_0$$
$$Q + (\alpha/2 - 2\beta)\omega + J_0(a)A = -G_T(\alpha^{1/2}) + I(\alpha^{1/2}) = R_1^S$$
$$\alpha\omega - aJ_1(a)A = -\alpha^{1/2}[dG_T(\alpha^{1/2})/dr - dI(\alpha^{1/2})/dr] = R_2^S. \tag{24}$$

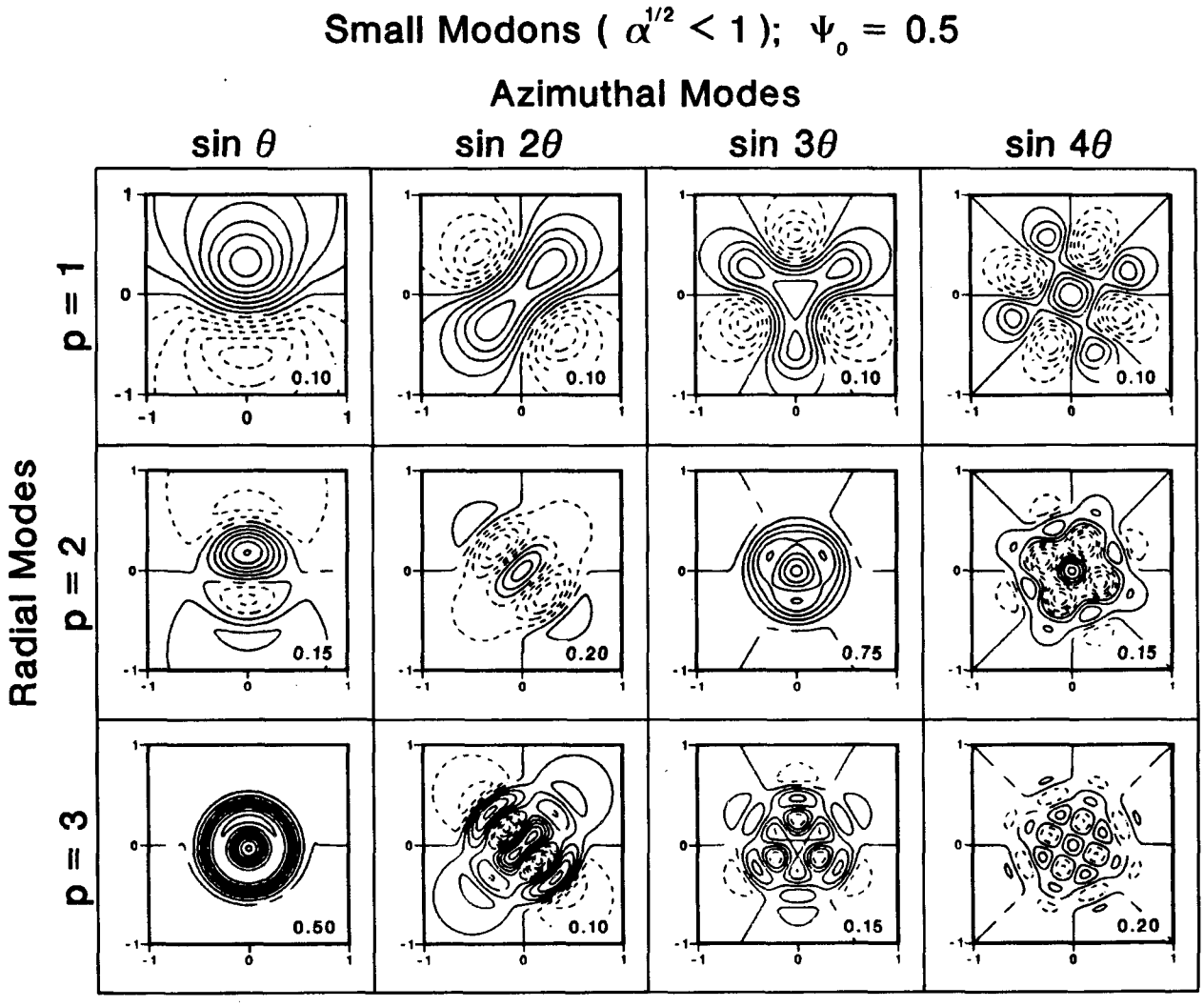

FIG. 3a. As in Fig. 2 but for $\Psi_0 = +0.5$.

The solution to (24) is straightforward:

$$Q\Delta_S = -\alpha\{(\Psi_0)[a(1/2 - 2a^{-2})J_1(a) + J_0(a)] + R_1^S[2a^{-1}J_1(a) - 1] + R_2^S[2a^{-2}J_0(a) + (1/2 - 2a^{-2})]\}$$
$$\omega\Delta_S = -\{aJ_1(a)(R_1^S - \Psi_0) + R_2^S[J_0(a) - 1]\}$$
$$A\Delta_S = \alpha(\Psi_0 - R_1^S + R_2^S/2), \quad (25)$$

where

$$\Delta_S = -\alpha[J_0(a) + (a/2)J_1(a) - 1]. \quad (26)$$

For parabolic topography, $G_T(r)$ and $I(r)$ are substantially simplified:

$$G_T(r) = -\beta\gamma(1 + 4\beta - r^2) \quad (27)$$
$$I(r) = (\gamma/4)[3/4 + \ln r - r^2(1 - r^2/4)]. \quad (28)$$

For this special case it is also found that

$$R_1^S = \gamma\{\beta(1 + 4\beta - \alpha) + (1/4)[3/4 + (1/2)\ln\alpha - \alpha(1 - \alpha/4)]\}$$
$$R_2^S = (\gamma/4)(1 - \alpha)^2 - 2\alpha\beta\gamma. \quad (29)$$

To summarize for $\alpha^{1/2} \leqslant 1$, the solution can be written as

$$\Psi^I = Q + \omega(r^2/2 - 2\beta) + AJ_0(\beta^{-1/2}r) + G_T(r) + b_n^I J_n(\beta^{-1/2}r)\sin n\theta, \quad r \leqslant \alpha^{1/2}$$
$$\Psi^{II} = I(r) + b_n^I \alpha^{n/2} J_n(a) r^{-n} \sin n\theta, \quad \alpha^{1/2} \leqslant r \leqslant 1$$
$$\Psi^{III} = b_n^I \alpha^{n/2} J_n(a) r^{-n} \sin n\theta, \quad 1 \leqslant r, \quad (30)$$

where $G_T(r)$, $I(r)$, Q, A, and ω are given, respectively, for general topography by (14) or (17), (23), and (25). For the special case of paraboloid topography ($m = 2$

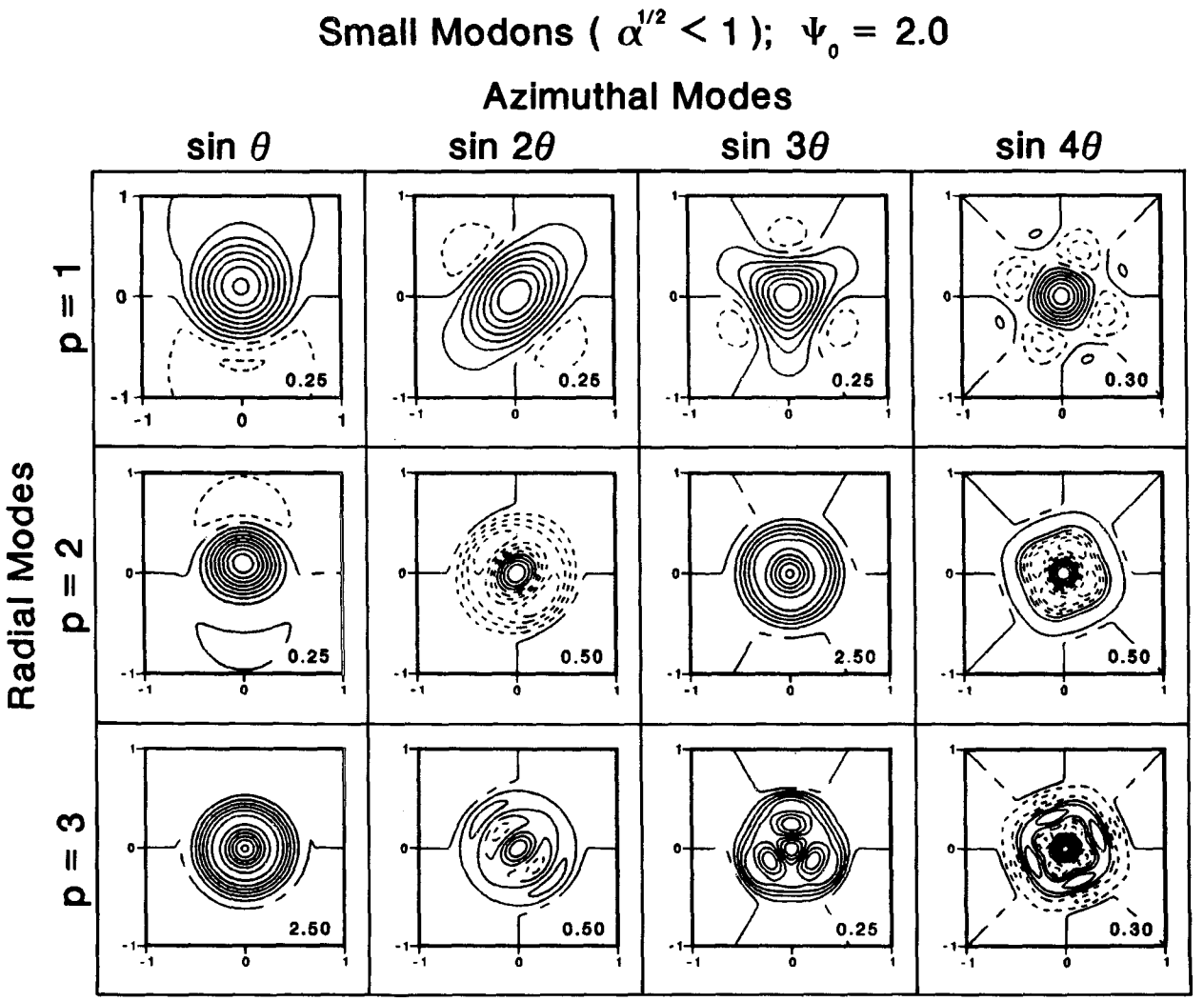

FIG. 3b. As in Fig. 2 but for $\Psi_0 = +2.0$.

in (7)), G_T and I are given by (27) and (28), while (29) can be used to simplify (25). Of course, in either case a is specified by $J_{n-1}(a) = 0$.

b. Large modon case ($\alpha^{1/2} \gg 1$)

Attention is now directed to the scenario $\alpha^{1/2} \gg 1$. Allowing for the possibility of independent separation constants for the two regions

$$r \gtrless 1,$$

the nondimensional version of (4) now takes the form

$$\nabla^2\Psi^I + \Psi^I/\beta_1 = -\gamma F(r) + (\omega r^2/2 + Q)/\beta_1, \quad r \leqslant 1$$
$$\nabla^2\Psi^{II} + \Psi^{II}/\beta_2 = (\omega r^2/2 + Q)/\beta_2, \quad 1 \leqslant r \leqslant \alpha^{1/2}$$
$$\nabla^2\Psi^{III} = 0, \quad \alpha^{1/2} \leqslant r. \tag{31}$$

Reference to Fig. 1 reveals that in both the large and small modon cases, region I describes the area where the modon lies over the seamount. Region III pertains to the flow external to the modon over a flat bottom, which is also relevant to both small and large modon cases. For these reasons, the general solutions for Ψ^I and Ψ^{III} are the same as in the previous scenario (9) except that β is now replaced by β_1 in the expression Ψ^I. For Ψ^{II} the general solution is readily found to be

$$\Psi^{II} = Q + \omega(-2\beta_2 + r^2/2) + [B_1 J_0(\beta_2^{-1/2}r) + B_2 Y_0(\beta_2^{-1/2}r)] + \sum_{n=1} [b_n^{II} J_n(\beta_2^{-1/2}r) + d_n^{II} Y_n(\beta_2^{-1/2}r)] \sin n\theta. \tag{32}$$

Since the functions J_0 and Y_0 occur in both the particular and homogeneous solutions, their amplitudes are determined by the patching conditions at $r = 1$ and $\alpha^{1/2}$, so B_1 and B_2 are yet to be determined.

We proceed as in section 3a and consider first the patch of azimuthal modes. As before, this results in four linear homogeneous equations for b_n^I, b_n^{II}, d_n^{II}, and b_n^{III}:

$$J_n(b)b_n^I - J_n(\beta_2^{-1/2})b_n^{II} - Y_n(\beta_2^{-1/2})d_n^{II} = 0$$
$$[-nJ_n(b) + bJ_{n-1}(b)]b_n^I + [nJ_n(\beta_2^{-1/2}) - \beta_2^{-1/2}J_{n-1}(\beta_n^{-1/2})]b_n^{II} + [nY_n(\beta_2^{-1/2}) - \beta_2^{-1/2}Y_{n-1}(\beta_2^{-1/2})]d_n^{II} = 0$$
$$J_n(a)b_n^{II} + Y_n(a)d_n^{II} - \alpha^{-n/2}b_n^{III} = 0$$
$$[-nJ_n(a) + \alpha J_{n-1}(a)]b_n^{II} + [-nY_n(a) + \alpha Y_{n-1}(a)]d_n^{II} + n\alpha^{-n/2}b_n^{III} = 0, \tag{33}$$

where

$$a = (\alpha/\beta_2)^{1/2}, \quad b = \beta_1^{-1/2}.$$

The consistency condition for (33) is

$$bJ_{n-1}(b)[J_n(\beta_2^{-1/2})Y_{n-1}(a) - J_{n-1}(a)Y_n(\beta_2^{-1/2})] + \beta_2^{-1/2}J_n(b)[J_{n-1}(a)Y_{n-1}(\beta_2^{-1/2}) - J_{n-1}(\beta_2^{-1/2})Y_{n-1}(a)] = 0. \tag{34}$$

Since β_1 and β_2 in general are independent, there are two obvious ways to satisfy (34). We select these parameters that

$$J_{n-1}(b) = 0$$
$$J_{n-1}(a)Y_{n-1}(\beta_2^{-1/2}) - J_{n-1}(\beta_2^{-1/2})Y_{n-1}(a) = 0. \tag{35}$$

The other choice,

$$J_n(b) = J_n(\beta_2^{-1/2})Y_{n-1}(a) - J_{n-1}(a)Y_n(\beta_2^{-1/2}) = 0,$$

is discarded since it does not resemble the small modon case.

Taking b_n^I as arbitrary, we can express the other coefficients in (33) as

$$b_n^{II} = (\pi/2)b_n^I\beta_2^{-1/2}J_n(b)Y_{n-1}(\beta_2^{-1/2})$$
$$d_n^{II} = -(\pi/2)\beta_2^{-1/2}b_n^I J_n(b)J_{n-1}(\beta_2^{-1/2})$$
$$b_n^{III} = \alpha^{(n-1)/2}b_n^I J_n(b)Y_{n-1}(\beta_2^{-1/2})/2Y_{n-1}(a). \tag{36}$$

The axisymmetric solution for Ψ^{II} is (from 32)

$$I = Q + \omega(r^2/2 - 2\beta_2) + [B_1 J_0(\beta_2^{-1/2}r) + B_2 Y_0(\beta_2^{-1/2}r)]. \tag{37}$$

The patch conditions (6) at $r = \alpha^{1/2}$ fix B_1 and B_2 so that (37) reduces to

$$I = \omega\{r^2/2 - 2\beta_2 - (\pi/2)[aY_1(a)(2\beta_2 - \alpha/2) - \alpha Y_0(a)]J_0(\beta_2^{-1/2}r) - (\pi/2)[\alpha J_0(a) + (\alpha/2 - 2\beta_2)aJ_1(a)]Y_0(\beta_2^{-1/2}r)\} + Q\{1 + (\pi a/2)[J_0(\beta_2^{-1/2}r)Y_1(a) - J_1(a)Y_0(\beta_2^{-1/2}r)]\}. \tag{38}$$

Now the rider condition $G_D(0) + A \equiv \Psi_0$ at $r = 0$ and the patch conditions at $r = 1$ yield the three simultaneous equations

$$Q - 2\beta_1\omega + A = \Psi_0$$
$$-N_1Q + [2(\beta_2 - \beta_1) - M_1]\omega + J_0(\beta_1^{-1/2})A = R_1^L$$
$$-N_2Q - M_2\omega - \beta_1^{-1/2}J_1(\beta_1^{-1/2})A = R_2^L, \tag{39}$$

where

$$M_1 = (\pi/2)\{[\alpha Y_0(a) + (\alpha/2 - 2\beta_2)aY_1(a)]J_0(\beta_2^{-1/2}) - [\alpha J_0(a) + (\alpha/2 - 2\beta_2)aJ_1(a)]Y_0(\beta_2^{-1/2})\}$$

$$M_2 = (\pi/2)\beta_2^{-1/2}\{[\alpha J_0(a) + (\alpha/2 - 2\beta_2)aJ_1(a)]Y_1(\beta_2^{-1/2}) - [\alpha Y_0(a) + (\alpha/2 - 2\beta_2)aY_1(a)]J_1(\beta_2^{-1/2})\}$$

$$N_1 = (\pi a/2)[J_0(\beta_2^{-1/2})Y_1(a) - J_1(a)Y_0(\beta_2^{-1/2})]$$

$$N_2 = (\pi a/2)(\beta_2^{-1/2})[J_1(a)Y_1(\beta_2^{-1/2}) - J_1(\beta_2^{-1/2})Y_1(a)]$$

$$R_1^L = -G_T(1)$$

$$R_2^L = -dG_T(1)/dr. \quad (40)$$

The solution of (39) is

$$Q\Delta_L = \Psi_0\{\beta_1^{-1/2}J_1(\beta_1^{-1/2})[M_1 - 2(\beta_2 - \beta_1)] + M_2J_0(\beta_1^{-1/2})\} - R_1^L\{2\beta_1^{1/2}J_1(\beta_1^{-1/2}) + M_2\} + R_2^L\{M_1 - 2(\beta_2 - \beta_1) - 2\beta_1J_0(\beta_1^{-1/2})\}$$

$$\omega\Delta_L = -\Psi_0[N_1\beta_1^{-1/2}J_1(\beta_1^{-1/2}) + N_2J_0(\beta_1^{-1/2})] + R_1^L[N_2 - \beta_1^{-1/2}J_1(\beta_1^{-1/2})] - R_2^L[J_0(\beta_1^{-1/2}) + N_1]$$

$$A\Delta_L = \Psi_0[\alpha + 2(\beta_2 - \beta_1)N_2] + R_1^L(M_2 + 2\beta_1N_2) + R_2^L[2(\beta_2 - \beta_1) - M_1 - 2\beta_1N_1], \quad (41)$$

where

$$\Delta_L = \alpha + 2(\beta_2 - \beta_1)[N_2 - \beta_1^{-1/2}J_1(\beta_1^{-1/2})] + \beta_1^{-1/2}J_1(\beta_1^{-1/2})M_1 + M_2J_0(\beta_1^{-1/2}) + 2\beta_1[\beta_1^{-1/2}J_1(\beta_1^{-1/2})N_1 + J_0(\beta_1^{-1/2})N_2].$$

In this last expression, we used the result

$$N_1M_2 - N_2M_1 = \alpha.$$

To summarize for $\alpha^{1/2} \geq 1$, the general solution is

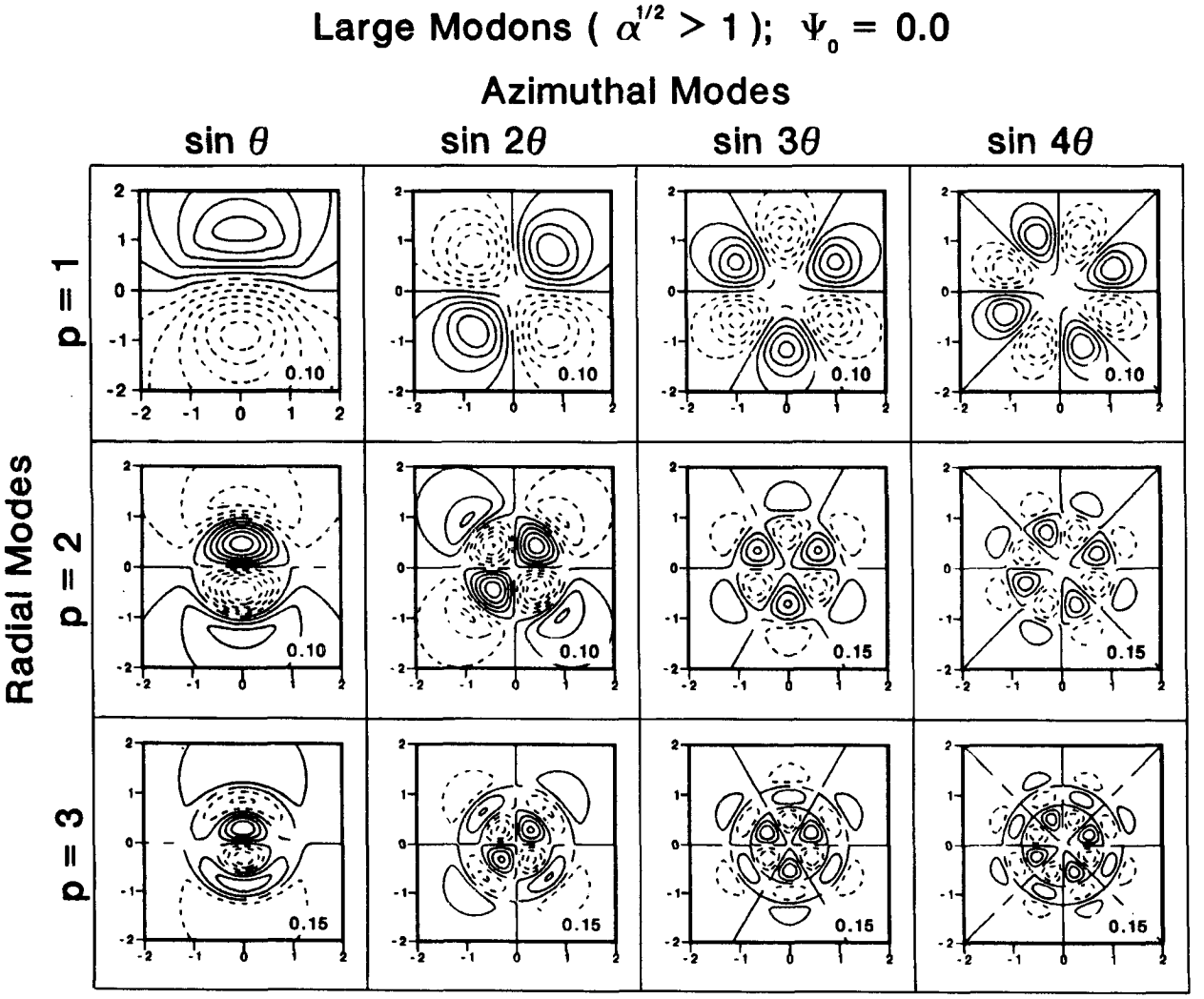

FIG. 4. Streamfunction (Ψ) contours for the large modon case ($\alpha = 2.0$) with $b_n^L = 1.0$, $\gamma = 0.25$ and no axisymmetric part ($\Psi_0 = 0$). The first four azimuthal modes ($\sin n\theta$, $n = 1, \cdots, 4$) and the three lowest-order radial modes ($p = 1, 2, 3$) are shown.

$$\Psi^I = [Q + \omega(r^2/2 - 2\beta_1)] + AJ_0(\beta_1^{-1/2}r) + G_T(r) + b_n^I J_n(\beta_1^{-1/2}r)\sin n\theta, \quad r \leq 1$$

$$\Psi^{II} = Q\{1 + (a\pi/2)[Y_1(a)J_0(\beta_2^{-1/2}r) - J_1(a)Y_0(\beta_2^{-1/2}r)]\} + \omega\{r^2/2 - 2\beta_2 - (\pi/2)[aY_1(a)(2\beta_2 - \alpha/2) - \alpha Y_0(a)] \times J_0(\beta_2^{-1/2}r)\} - (\pi/2)[\alpha J_0(a) + aJ_1(a) \times (2\beta_2 - \alpha/2)]Y_0(\beta_2^{-1/2}r)\} + [b_n J_n(\beta_2^{-1/2}r) + d_n Y_n(\beta_2^{-1/2}r)]\sin n\theta, \quad 1 \leq r \leq \alpha^{1/2}$$

$$\Psi^{III} = b_n^{III} r^{-n}\sin n\theta, \quad \alpha^{1/2} \leq r, \qquad (42)$$

where b_n^{II}, d_n^{II}, and b_n^{III} are given by (36) and Q, ω, and A are given by (41). Also, the consistency relation is (35).

It is straightforward to show that Ψ^{II} vanishes when $\alpha^{1/2} = 1$, so that both large and small modon solutions give the same result when $\alpha^{1/2} = 1$.

When $\beta_1 = \beta_2 = \beta$ and $m = 2$ [parabolic topography in (7)], some simplification of these results occurs. In particular, the consistency relation (34) reduces to

$$J_{n-1}(a) = 0. \qquad (43)$$

This is the same as (20) except that the $\alpha^{1/2}$ in a is larger than 1. Also $\beta_1 = \beta_2$ simplifies (36) to

$$b_n^{II} = b_n^I$$

$$d_n^{II} = 0$$

$$b_n^{III} = \alpha^{n/2} J_n(a) b_n^I.$$

Noting that

$$\beta^{-1/2}J_1(\beta^{-1/2})M_1 + J_0(\beta^{-1/2})M_2 = -[\alpha J_0(a) + (\alpha/2 - 2\beta)aJ_1(a)],$$

$$\beta^{-1/2}J_1(\beta^{-1/2})N_1 + J_0(\beta^{-1/2})N_2 = -aJ_1(a),$$

and

$$\Delta_L = \alpha[1 - J_0(a) - (a/2)J_1(a)] = \tilde{\Delta}_L$$

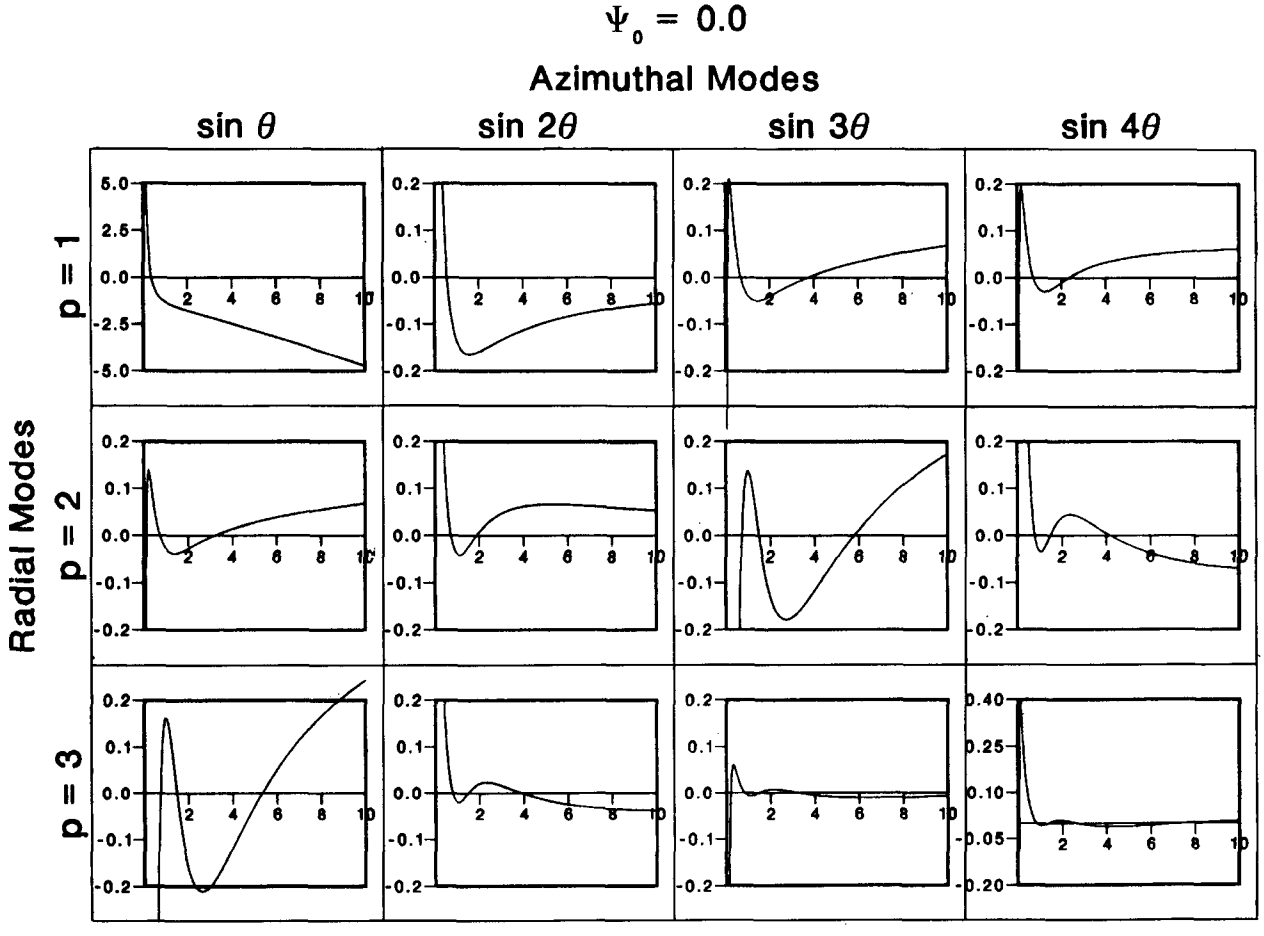

FIG. 5a. Dispersion relation $\omega = \omega(\alpha, \Psi_0)$ with $\Psi_0 = 0$ and $\gamma = 0.25$.

it is seen that for the parabolic topography case (41) reduces to

$$Q\tilde{\Delta}_L = -\Psi_0[\alpha J_0(a) + a(\alpha/2 - 2\beta)J_1(a)] - 2\beta\gamma[(M_1 - 2\beta J_0(\beta^{-1/2})] - 4\beta^2\gamma[M_2 + 2\beta^{1/2}J_1(\beta^{-1/2})]$$

$$\omega\tilde{\Delta}_L = \Psi_0 aJ_1(a) + 2\beta\gamma[N_1 + J_0(\beta^{-1/2})] + 4\beta^2\gamma[N_2 - \beta^{-1/2}J_1(\beta^{-1/2})]$$

$$A\tilde{\Delta}_L = \alpha\Psi_0 + 4\beta^2\gamma(M_2 + 2\beta N_2) + 2\beta\gamma(M_1 + 2\beta N_1). \quad (44)$$

The solution (42) then reduces to

$$\Psi^I = [Q + \omega(r^2/2 - 2\beta)] + \gamma[-\beta(1 + 4\beta) + \beta r^2] + AJ_0(\beta^{-1/2}r) + b_n^I J_n(\beta^{-1/2}r)\sin n\theta, \quad r \leq 1$$

$$\Psi^{II} = Q\{1 + (\pi a/2)[Y_1(a)J_0(\beta^{-1/2}r) - J_1(a)Y_0(\beta^{-1/2}r)]\} + \omega\{r^2/2 - 2\beta - (\pi/2)[aY_1(a)(2\beta - \alpha/2) - \alpha Y_0(a)]J_0(\beta^{-1/2}r)] - (\pi/2)[\alpha J_0(a) + (\alpha/2 - 2\beta)aJ_1(a)]Y_0(\beta^{-1/2}r)]\} + b_n^I J_n(\beta^{-1/2}r)\sin n\theta, \quad 1 \leq r \leq \alpha^{1/2}$$

$$\Psi^{III} = \alpha^{n/2}J_n(a)b_n^I r^{-n}\sin n\theta, \quad \alpha^{1/2} \leq r. \quad (45)$$

In this case Q, ω, and A are given by (44), and the consistency relation is $J_{n-1}(a) = 0$.

4. Discussion

The modon solutions outlined in sections 2 and 3 differ in two fundamental ways from those in most prior studies. First, the background medium is discontinuous as the topography has compact support (Fig. 1). This contrasts with the uniform infinite beta plane used in most modon studies. Even in the prior studies of modon propagation over topography, the topography was a smoothly varying function of position without compact support. It must be noted, however, that the inclusion of topography ($\gamma \neq 0$) in the problem merely produces an axisymmetric flow with a specified

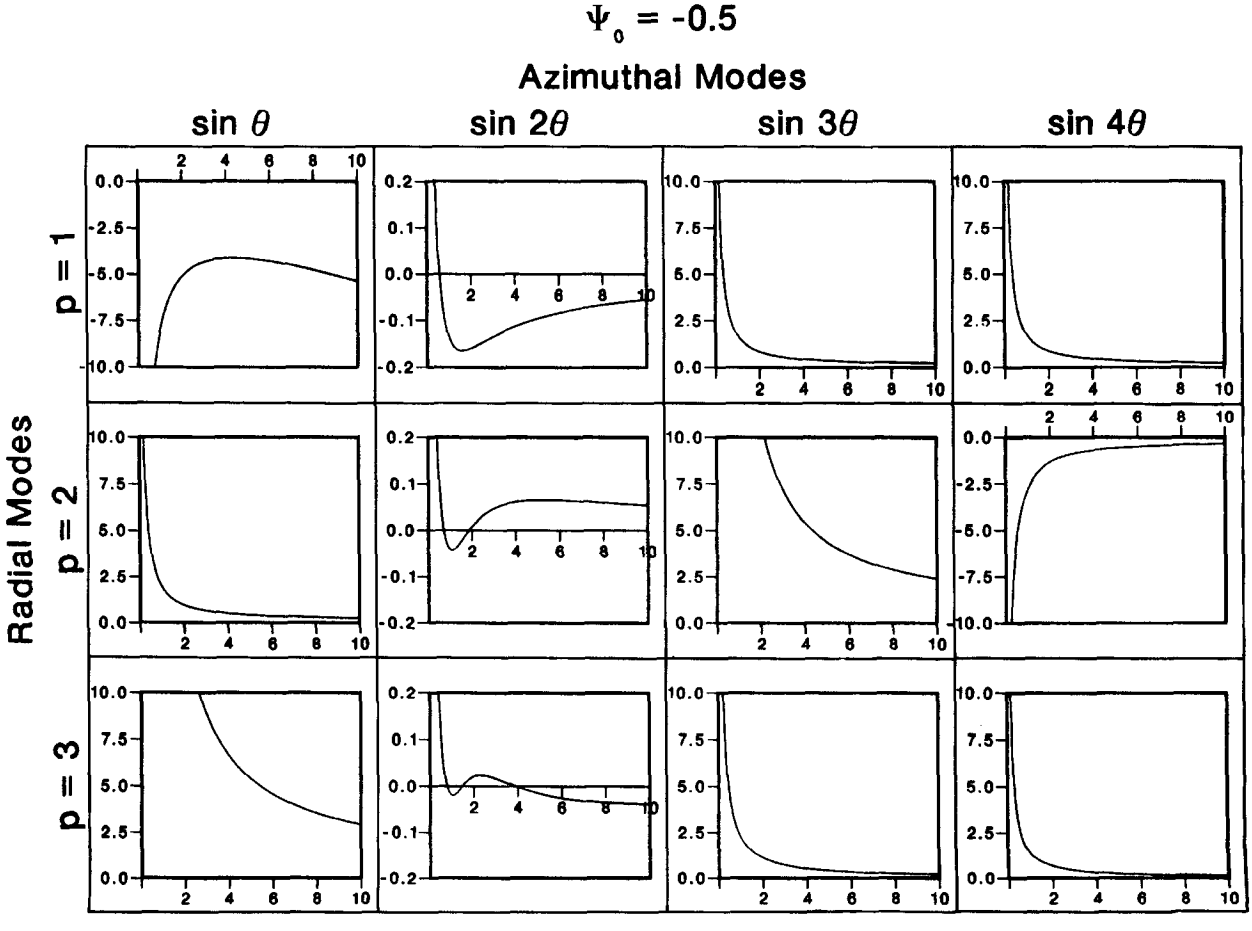

FIG. 5b. Dispersion relation with $\Psi_0 = -0.5$ and $\gamma = 0.25$.

form and amplitude [i.e., the functions I and G_T in Eq. (17), (18), or (37)]. Without topography ($\gamma = 0$), there is still an axisymmetric flow, but the values of ω, A, and Q depend only upon the rider value Ψ_0.

Second, all cases considered previously deal with modon motion that was essentially rectilinear. The search for a solution that transports fluid in a steadily translating frame requires the existence of a bounding streakline $\Psi + Ua \sin\theta = \text{const}$ (Flierl et al. 1980). It is important to stress that the bounding streakline concept has no direct analog in our steadily rotating frame. That is, our solution need not necessarily involve a dividing streakline that separates an outer and an inner region that is transporting fluid. Instead, the solution sought specifies only that the inner and outer streamfunction fields be continuous along $r = r_a$. It is emphasized that we do not require this curve to be a streamline.

In the present case, there are three solution regions, and we also impose the continuity of Ψ, $\partial\Psi/\partial r$, and $\partial\Psi/\partial\theta$ at the two dividing circles separating these regions but do not require the vorticity to be continuous across the line. Although this constitutes a more general solution class, the relaxation of the requirement for continuous vorticity has the consequence that the modon amplitude (b_n^I) is unspecified and so is a free parameter. In a more pragmatic sense, continuity of the vorticity at both (or only one) radial boundaries would overspecify the conditions on the constants b_n^I, b_n^{II}, b_n^{III}, and c_n^{II} (or d_n^{II}) in section 3.

The nonlinear forms treated in this work rotate steadily about a central point. As such, they are somewhat reminiscent of Reznik's (1985) modon dipole eddy pair, which orbits steadily around a line of constant height along parabolic topography of infinite extent. Reznik's solution and ours, however, are unrelated, since in his case the modon changes to a monopole when the orbit radius of the modon is reduced to zero.

There is a great variety of different streamfunctions for the small modon case ($\alpha^{1/2} < 1$). Figure 2 is a matrix that represents the different azimuthal modes ($\sin n\theta$, $n = 1, 2, \cdots$) and different radial modes ($J_{n-1}(a) = 0, p = 1, 2, \cdots$) that arise from the countable infinity of solutions to (20) when $\Psi_0 = 0$. The progressively increasing complexity of the streamfunctions is evident as the azimuthal mode number (n) or the radial root number (p), or both, are increased.

While the different azimuthal and radial modes shown in Fig. 2 are noteworthy for their variety, the

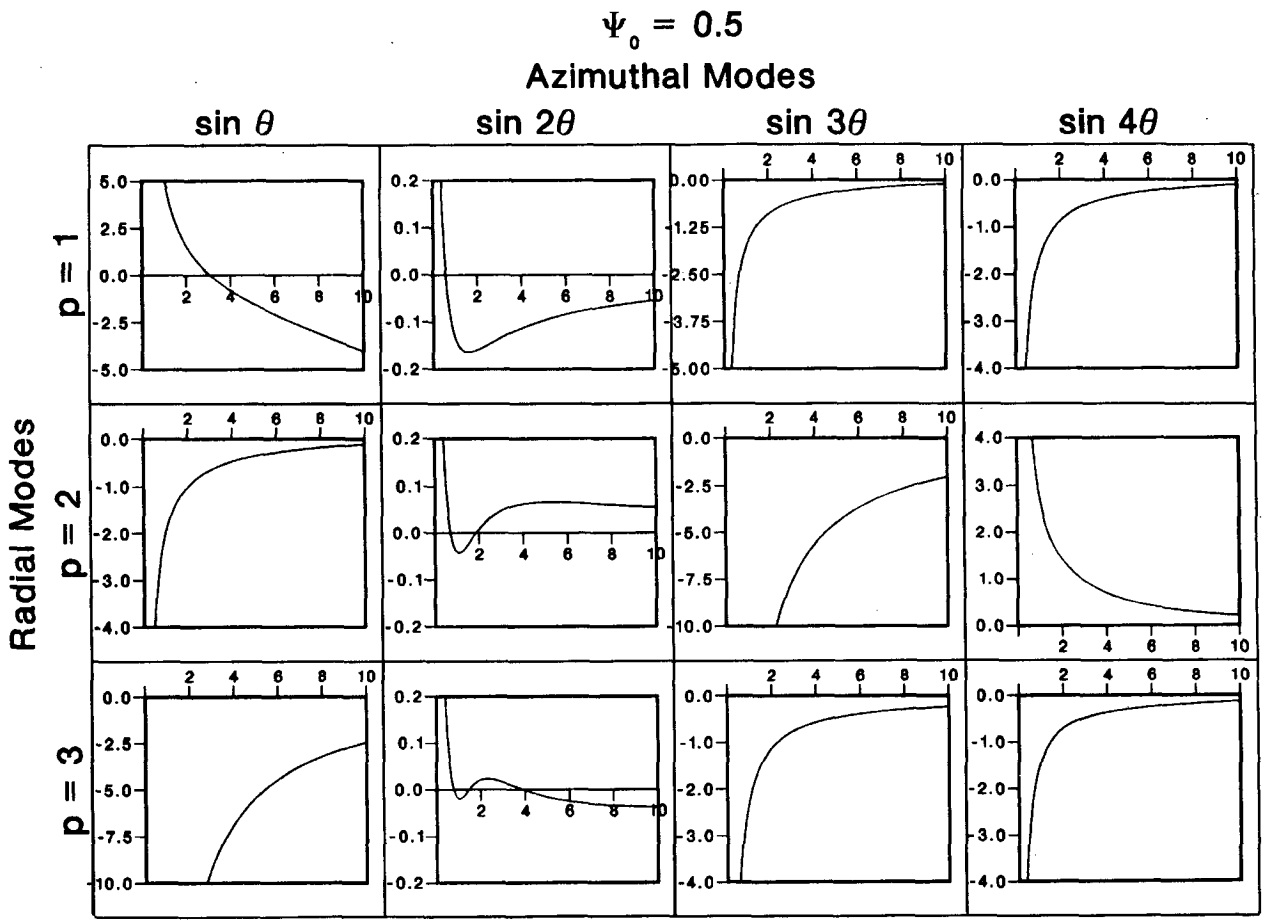

FIG. 5c. Dispersion relation with $\Psi_0 = +0.5$. In each case $\gamma = +0.25$.

introduction of nonzero values of Ψ_0 in the axisymmetric part of the solution provides some exceptionally interesting variants of these figures. In Figs. 3a,b, we show streamfunction contours identical to those in Fig. 2 but with $\Psi_0 = 0.5$ and 2.0, respectively. As Ψ_0 is increased from the zero value shown in Fig. 2, anticyclonic values of Ψ are enhanced and cyclonic Ψ values are cancelled by positive Ψ_0. Some of the resulting forms are quite interesting. For example, the $\sin\theta$ column in Fig. 3b shows that for the first radial root ($p = 1$) the dipole shifts to a near-anticyclonic monopole with a weak cyclonic outlying vortex. The $p = 2$ case for $\sin\theta$ also shows the way in which a quadrupole can change to essentially a monopole with weak attached vortices. Perhaps the most striking form, however, is the $p = 1$, $\sin 2\theta$ case. What begins with $\Psi_0 = 0$ in Fig. 2 as a quadrupole can be seen to become essentially a compactly structured tripole in Fig. 3b, with the addition of a sufficiently large anticyclone ($\Psi_0 = 2.0$ here).

The large modon case ($\alpha^{1/2} > 1$) shows the same rich variety present in the small modon case (Fig. 4). Moreover, there is a qualitative similarity between this large case and the small case shown in Fig. 2. That there should be at least a superficial similarity between the two cases is not surprising. They both have the same azimuthal structure ($\sin n\theta$) and their radial mode structures are both determined by the same eigenvalue relation $J_{n-1}(a) = 0$. In addition, the two solutions reduce to the same form at the intersection point $\alpha = 1$, that is, when the modon is precisely as large as the mountain.

The two cases shown in Figs. 2 and 4 and treated in sections 2 and 3 come about because we must allow for the modon radius to be smaller or larger than the radial extent of the mountain (see Fig. 1). In the small modon case ($\alpha^{1/2} < 1$), the modon lies wholly over the mountain and the vortex stretching constituent of the potential vorticity has continuous radial derivatives at $r = \alpha^{1/2}$ (the modon radius). For the large modon case ($\alpha^{1/2} > 1$), the modon extends beyond the edge of the mountain and the topography is not continuously differentiable at $r = 1$. Because of these fundamentally different scenarios, the solutions for $\alpha^{1/2} \gtrless 1$ in the annular region II are quite different [Eq. (30) vs Eq. (45)].

TABLE 1. A comparison of the properties of the rigid-lid, beta-plane modon of Larichev and Reznik (1976) with the properties of those in the present work.

Rectilinear modons (Larichev and Reznik 1976)	Topographic modons (this study)
1. $\Psi = \sin\theta$ is basic modon	$\Psi = \sin n\theta$ ($n > 1$) is basic modon
2. *P.V.* $- \Psi$ relation defined in two regions	*P.V.* $- \Psi$ relation defined in three regions
3. Straight-line motion	Rotary motion
4. Only translate eastward in the rigid-lid model.	May rotate clockwise or anticlockwise
5. Translation speed independent of axisymmetric part	Rotation rate (ω) dependent upon axisymmetric amplitude
6. Riders have form $\sin n\theta$, ($n = 0$ and $n \geq 2$) and $\cos n\theta$, ($n \geq 1$)	Axisymmetric riders only

In view of these different functional forms, it is interesting to note that the dispersion relations, $\omega = \omega(\alpha; \Psi_0)$, for each of these modes (Figs. 5a–c) are continuous at $\alpha = 1$. Moreover, calculation reveals that the first derivative of ω is continuous across $\alpha = 1$, and this accounts for the smoothness in the profiles at $\alpha = 1$. From (25) and (44) it is seen that ω has a term that is proportional to γ. For the case of no topography ($\gamma = 0$) ω is a well-behaved function of α. It is worth noting that only for the $n = 2$ case $\omega \equiv 0$ when $\gamma = 0$.

Figures 5a–c show the dispersion relations (plotted as ω/γ for convenience) for the radial and azimuthal modes when $\Psi_0 = 0$, -0.5, and 0.5. That is, the rotational frequency is depicted as a function of modon size (α) for superimposed axisymmetric circulations that are, respectively, zero, cyclonic, and anticyclonic. A number of trends are immediately obvious. The first is that for many of the modes, and especially for the $\Psi_0 = 0$ case, ω/γ may be either negative or positive. A mode may rotate clockwise ($\omega/\gamma < 0$) or anticlockwise ($\omega/\gamma > 0$), depending only upon its size (α).

In the event that an axisymmetric cyclonic rider is imposed upon the flow ($\Psi_0 = -0.5$, Fig. 5b), the waves are, in general, shifted upward (ω/γ becomes more positive). The addition of an anticyclonic rider ($\Psi_0 = +0.5$, Fig. 5c) produces the opposite effect; that is, ω/γ becomes more negative and the modons generally favor clockwise rotation (ω/γ more negative). A conspicuous violation of this trend occurs for the $\sin 2\theta$ modons that are unaffected by the addition of an axisymmetric vortex. Reference to the dispersion relations for small and large modons [the ω solutions in (25) and (44), respectively] indicates that Ψ_0 and $J_1(a)$ always occur as a product. The dispersion relation for this mode is $J_1(a) = 0$, which nullifies the effect of adding any axisymmetric part.

The possibility of positive and negative rotation rates for any particular mode and the sensitivity of ω/γ to Ψ_0 occur because the rotation direction and angular velocity of these modons are determined by three factors:

- mutual advection of the vortices
- the magnitude and sign of γ
- the presence of an arbitrary axisymmetric vortex.

The interplay between these effects gives a richness of behavior that is not available with the rigid-lid beta-plane modon (Larichev and Reznik 1976), which can only propagate eastward.

The final point to be made on the dispersion relations in Fig. 5 is that they are all singular at $\alpha = 0$. Equation (25), indicates that the small α behavior is given by $\omega/\gamma \propto \pm \ln\alpha/\alpha$. For small scales, however, the QG model is inappropriate and other physics should be included.

Since the rotating modons described in this work are new and offer such rich and varied behavior, it is appropriate to compare various facets of their behavior with that of the classical Larichev and Reznik (1976) rectilinear case. This is summarized in Table 1.

5. Conclusions

We have analyzed the structure and properties of steadily rotating modon solutions to the quasigeostrophic equations of motion over isolated topography. The following conclusions can be made:

- Steady closed-form solutions are possible with quadratic topography and have an azimuthal structure characterized by $\sin n\theta$ ($n = 1, 2, 3, \cdots$).
- Each $\sin n\theta$ azimuthal mode has a countable infinity of radial modes.
- Both cyclonically and anticyclonically rotating solutions are possible.
- Solutions are valid for seamounts, flat bottoms, or depressions ($\gamma \gtrless 0$).
- An axisymmetric vortex rider of arbitrary amplitude (Ψ_0) can be superimposed on these solutions, and its inclusion strongly influences the angular velocity of the modon.
- The case $n = 2$ and no topography ($\gamma = 0$) yields $\omega = 0$. When an axisymmetric rider is present ($\Psi_0 \neq 0$) the solutions are tripolar; see Figure 3a,b. Hence, tripoles over flat topography do not rotate in this model.

This paper has only addressed some elementary theoretical properties of rotating modons. The results suggests many other questions that can be resolved only after further study. In our view, the two most pressing are as follows:

- *Generation.* A viable generation mechanism for rotating modons is unknown. If one were found, the lowest order ($\sin\theta, p = 1$) would have an unambiguous, periodic signal that might be stable and observable for extended periods of time.
- *Stability.* It seems likely that the large p, large n modons would be unstable, as might the small p, small n ones with large amplitude ($b_n^I \gg 0$). Theoretical and diagnostic studies along the lines reported by Butchart et al. (1989) as well as numerical experiments should resolve this.

Acknowledgments. R. P. Mied and G. L. Lindemann acknowledge support from the Naval Research Laboratory Project 51-2914-00. A. D. Kirwan acknowledges the support of ONR Grant N00014-89-J-1595 (Office of Naval Research) and the Samuel L. and Fay M. Slover endowment to Old Dominion University. We are particularly grateful to Vitaly Larichev and Sue Ellen Haupt for their valuable critiques as reviewers. Glen Wheless and John Kroll also provided us with some useful criticisms. Finally, the authors are grateful to Julie Rea for exceptional tenacity in typing several drafts of this work.

REFERENCES

Bender, C. M., and S. A. Orszag, 1978: *Advanced Mathematical Methods for Scientists and Engineers.* McGraw-Hill, 593 pp.

Berestov, A. L., 1979: Solitary Rossby waves. *Izv. Atmos. Ocean Phys.*, **15,** 443–447.

Butchart, N., K. Haines, and J. C. Marshall, 1989: A theoretical and diagnostic study of solitary waves and atmospheric blocking. *J. Atmos. Sci.*, **46,** 2063–2078.

Carnevale, G. F., G. K. Vallis, and R. Purini, 1988: Propagation of barotropic modons over topography. *Geophys. Astrophys. Fluid Dyn.*, **41,** 45–101.

Flierl, G. R., V. D. Larichev, J. C. McWilliams, and G. M. Reznik, 1980: The dynamics of baroclinic and barotropic solitary eddies. *Dyn. Atmos. Oceans,* **5,** 1–41.

——, M. E. Stern, and J. A. Whitehead, 1983: The physical significance of modons: Laboratory experiments and general integral constraints. *Dyn. Atmos. Oceans,* 7, 233–263.

Haines, K., 1989: Baroclinic modons as prototypes for atmospheric blocking. *J. Atmos. Sci.*, **46,** 3202–3218.

Hobson, D. D., 1991: A point vortex dipole model of an isolated modon. *Phys. Fluids A3,* **12,** 3027–3033.

Kloosterzeil, R. C., and G. J. F. van Heijst, 1991: An experimental study of unstable barotropic vortices in a rotating fluid. *J. Fluid. Mech.*, **22,** 1–24.

Larichev, V. D., and G. M. Reznik, 1976: Two dimensional Rossby solutions: An exact solution. *Polymode News,* **19,** 3.

——, and ——, 1982: Numerical experiments on the study of collisions of two-dimensional solitary Rossby waves. *Dokl. Akad. Nauk SSSR,* **264,** 229–233.

——, and ——, 1983: On collisions between two-dimensional Rossby waves. *Oceanology,* **23,** 545–552.

Makino, M., T. Kamimara, and T. Taniuti, 1981: Dynamics of two-dimensional solitary vortices in a low-β plasma with convective motion. *J. Phys. Soc. Japan,* **50,** 980–989.

McWilliams, J. C., 1980: An application of equivalent modons to atmospheric blocking. *Dyn. Atmos. Oceans,* **5,** 43–66.

——, 1983: Interactions of Isolated Vortices: II. Modon generation by monopole collision. *Geophys. Astrophys. Fluid Dyn.*, **24,** 1–22.

——, and G. R. Flierl, 1979: On the evolution of isolated, nonlinear vortices. *J. Phys. Oceanogr.*, **9,** 1155–1182.

——, and N. J. Zabusky, 1982: Interactions of isolated vortices: I. Modons colliding with modons. *Geophys. Astrophys. Fluid Dyn.*, **19,** 207–227.

——, G. R. Flierl, V. D. Larichev, and G. M. Reznik, 1981: Numerical studies of barotropic modons. *Dyn. Atmos. Oceans,* **5,** 219–238.

Mied, R. P., and G. J. Lindemann, 1982: The birth and evolution of eastward-propagating modons. *J. Phys. Oceanogr.*, **12,** 213–230.

Nof, D., 1990: Modons and monopoles on a gamma-plane. *Geophys. Astrophys. Fluid Dyn.*, **52,** 71–87.

Reznik, G. M., 1985: Exact solution for two-dimensional topographic Rossby solution. *Dok. Akad. Nauk SSSR,* **282,** 981–985 (in Russian).

Swaters, G. E., 1986: Barotropic modon propagation over slowly varying topography. *Geophys. Astrophys. Fluid Dyn.*, **36,** 85–113.

——, and G. R. Flierl, 1989: Ekman dissipation of a barotropic modon. *Mesoscale/Synoptic Coherent Structures in Geophysical Turbulence.* J. C. J. Nihoul and B. M. Jamart, Eds.,

Stern, M. E., 1975: Minimal properties of planetary eddies. *J. Mar. Res.*, **33,** 1–13.

Tribbia, J. J., 1984: Modons in spherical geometry. *Geophys. Astrophys. Fluid Dyn.*, **30,** 131–168.

Verkley, W. T. M., 1984: The construction of barotropic modons on a sphere. *J. Atmos. Sci.*, **41,** 2492–2504.

——, 1987: Stationary barotropic modons in westerly background flows. *J. Atmos. Sci.*, **44,** 2383–2398.